Self-diffusion of iron in amorphous iron nitride

Mukul Gupta,[1] Ajay Gupta,[1,*] S. Rajagopalan,[2] and A. K. Tyagi[2]
[1]*Inter-University Consortium for DAE facilities, Khandwa Road, Indore-452 017, India*
[2]*Materials Science Division, Indira Gandhi Center for Atomic Research, Kalpakkam-603102, India*
(Received 11 September 2001; revised manuscript received 8 January 2002; published 6 June 2002)

The measurement of self-diffusion of iron in amorphous $FeN_{0.7}$ using secondary-ion mass spectroscopy is reported. Diffusion broadening of tracer layers of $^{57}FeN_{0.7}$ was observed after isothermal vacuum annealing of the films at different temperatures. Strong structural relaxation effects on diffusion coefficient were observed below crystallization temperature of the amorphous phase. In the well-relaxed state, the values of preexponential factor D_0 and activation energy q are given by $\ln D_0 = -16.6 \pm 2$ m^2/s and $q = 1.3 \pm 0.2$ eV. On the basis of correlation between $\ln D_0$ and q, it is suggested that the mechanism of self-diffusion of iron in amorphous iron nitride is very similar to that in metallic glasses.

DOI: 10.1103/PhysRevB.65.214204 PACS number(s): 66.30.Fq

Diffusion in amorphous alloys has been of great interest, as changes in the structure of these alloys and their relation to the physical and mechanical properties are of primary interest from the point of view of their technological application and stability against external environment. Despite extensive studies in recent years,[1–7] the underlying mechanism of diffusion in amorphous alloys has not yet been understood properly. While in crystalline solids atomic diffusion is known to take place involving point defects and thermally activated jumps, the diffusion in equilibrium liquids involves the collective motion of a group of atoms. The situation in an amorphous system, which can be construed as a supercooled liquid, is not very clear. In covalent glasses the existence of point defects is well established; therefore the diffusion mechanism is expected to be similar to crystalline solids. On the other hand, in amorphous alloys the structural defects are expected to be more diffused in nature, characterized by an excess free volume.[8]

Available results on atomic diffusion in amorphous alloys do not provide a uniform picture of the diffusion mechanism and more often seem to be conflicting. While some results point towards single jump mechanism analogous to vacancy diffusion in crystals,[2,3] several others suggest a highly collective mechanism involving a large number of atoms.[4,7] Effects of hydrostatic pressure and the isotope effect have been very helpful in elucidating the mechanism of diffusion in these systems. In the case of impurity diffusion in metallic glasses, several factors such as atomic size mismatch and chemical affinity between impurity and host atoms affect the atomic diffusion in metallic glasses significantly. Therefore study of self-diffusion in metallic glasses has been particularly useful in elucidating the mechanism responsible.[9–12] Most extensive studies have been done on metal-metal metallic glasses such as Co-Zr[1], Ni-Zr[3], etc., while relatively fewer studies exist on transition-metal–metalloid (TM-M) systems.[6,13,14]

In view of the rather obscure picture of the diffusion mechanism in amorphous alloys it would be interesting to extend these studies to some unconventional amorphous alloy systems. In some such studies, atomic diffusion in recently discovered bulk metallic glasses has been reported.[15–17] In the present study we report measurements of self-diffusion of iron in the amorphous $FeN_{0.7}$ alloy, prepared by reactive ion-beam sputtering.[18] This system may have a local structure very different from that in conventional metallic, glasses. Metal-metal metallic glasses in the absence of any directional bond are expected to have a local structure closer to the dense-random packing model. In comparison, in metal-metalloid systems the metalloids have covalent directional bonds with metals, resulting in a rather well-defined short-range order around metalloid atoms.[19] In the extreme case of covalent glasses the existence of localized defects is well established; therefore it may be interesting to see the effect of strong covalent bonds in the Fe-N alloy system on atomic diffusion. The Fe-N bonds are known to be one of the strongest covalent bonds. Furthermore, the higher nitrogen stoichiometry of $FeN_{0.7}$ means a higher density of covalent bonds. Therefore diffusion studies in this system are expected to provide additional insight into the diffusion mechanism in amorphous alloys.

Iron nitride thin films were deposited by reactive ion-beam sputtering of iron with a beam of nitrogen ions using a 3-cm broad-beam Kaufman-type hot-cathode ion gun with a base vacuum of better than 1×10^{-7} Torr. A nitrogen (purity 99.9995%) ion beam of about 800 eV and 90 mA was obtained from the ion source and kept constant throughout the deposition. The deposition was carried out at room temperature. The target was kept at an angle of about 45° with respect to the incident ion beam, and the substrates were kept at a distance of about 120 mm from the target in a direction normal to the ion beam. Earlier studies have shown that the nitride formed under these conditions is amorphous in nature and has a stoichiometry of $FeN_{0.7}$. The Mössbauer pattern of the present specimen is identical to that obtained in the earlier study,[18] thus confirming that the stoichiometry in the present film is $FeN_{0.7}$. For the diffusion measurements a five-layer structure consisting of nominal thickness in the order [float glass (substrate) | $^{nat}FeN_{0.7}$ (450 Å) | $^{57}FeN_{0.7}$ (35 Å) | $^{nat}FeN_{0.7}$ (500 Å) | $^{57}FeN_{0.7}$ (35 Å) | $^{nat}FeN_{0.7}$ (500 Å)] was deposited. The two tracer layers of $^{57}FeN_{0.7}$ with known separation helped in the calibration of the sputtering rate and hence the depth scales during secondary-ion mass spectrometry (SIMS) measurements.

Thickness measurements and structural characterization

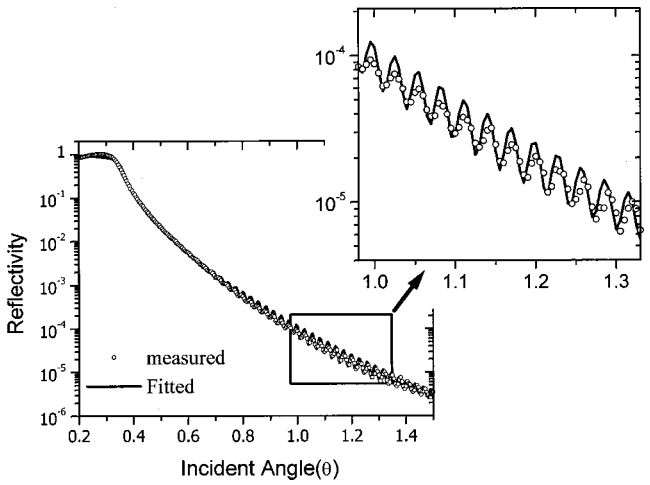

FIG. 1. Grazing-incidence x-ray reflectivity pattern of the as-deposited film. The thickness of the film calculated from the period of oscillations is 1450 Å.

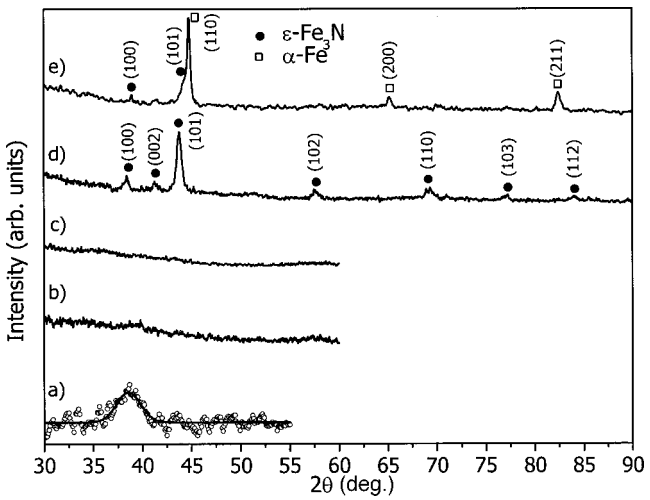

FIG. 2. The grazing-incidence x-ray diffraction pattern of the film (a) as-deposited on silicon substrate, (b) as-deposited on glass substrate, and (c) annealed in vacuum at 523 K, (d) at 593 K, and (e) at 723 K. The counting time per step for the pattern (a) was 60 times more than other patterns.

of the film were done by grazing incidence x-ray reflectivity (XRR) and grazing-incidence x-ray diffraction (GIXRD) using a Siemens-D5000 diffractometer (Cu $K\alpha$ x rays) with a thin-film attachment. The reflectivity pattern of the as-deposited film is shown in Fig. 1. The period of oscillations gives the total thickness of the film with an accuracy of ± 1 Å. The reflectivity pattern was fitted using a computer program based on Parratt's formalism[20] and the thickness of the film was found to be 1450 ± 1 Å as compared to the nominal thickness of 1520 Å. Thus the actual structure of the film is [float glass (substrate) | $^{nat}FeN_{0.7}$ (435 Å) | $^{57}FeN_{0.7}$ (32 Å) | $^{nat}FeN_{0.7}$ (475 Å) | $^{57}FeN_{0.7}$ (32 Å) | $^{nat}FeN_{0.7}$ (475 Å)]. The roughness of the top surface of the film is 12 ± 0.5 Å as compared to substrate roughness of 9 ± 0.5 Å. A detailed fitting of the GIXRR pattern shows that there is no electron density contrast between ^{nat}FeN and ^{57}FeN layers; therefore the stoichiometry of the marker layers is the same as that of the bulk of the film. The mass density of the film was obtained using the known stoichiometry and the value of critical angle for total external reflection of x rays as obtained from the wavelength-dependent XRR measurements.[18] The density of the film in the as-deposited state is 6.2 g/cm^3, which increases up to a value of 6.5 g/cm^3 after annealing at 523 K for 40 min.

The diffraction pattern of as-deposited film is shown in Figs. 2(a) and 2(b). The pattern indicates that the film is amorphous in structure. Figure 2(a) shows the diffraction pattern of the as-deposited film on a silicon substrate taken with higher statistics. The broad hump at $2\theta = 38.7°$ characteristic of an amorphous phase is clearly visible. This corresponds to an average Fe-Fe nearest-neighbor distance of $a = 1.23\lambda/2 \sin\theta = 2.86$ Å.[21] It may be noted that generally in transition-metal–metalloid (TM-M) glasses, having composition around eutectic ($TM_{80}M_{20}$), a broad hump appears around $2\theta = 44° - 45°$. A larger Fe-Fe nearest-neighbor distance in the present case may be attributed to a larger nitrogen content. The crystallization of the film was studied by isochronal annealing of the film at different temperatures. From the figure it can be seen that there is no change in the x-ray diffraction (XRD) pattern up to a temperature of 523 K. This indicates that the amorphous film is stable at least up to 523 K. Further annealing of the film at 593 K causes crystallization, and the phase formed is identified as ϵ-Fe_3N. After annealing at 723 K pure α-Fe becomes the dominant phase.

The conversion electron Mössbauer spectrum (CEMS) of the film is shown in Fig. 3. The as-deposited film shows an asymmetric doublet, which is fitted by deconvoluting it into four subspectra[18,22] as given in Table I. After annealing at 523 K there is no qualitative change in the Mössbauer spectrum, and it still consists of four subspectra—two doublets and two singlets. This suggests that the specimen is still in the amorphous state. There are small changes in the hyperfine field parameters and relative areas of various subspectra as given in Table I, which may be attributed to some structural relaxation in the sample. As will be seen later, structural relaxation is also evident from the variation of diffusivity with annealing time at a given temperature. After annealing at 593 K the spectrum transforms into a broad sextet with its hyperfine parameters corresponding to ϵ-Fe_3N. Further annealing at 723 K results in development of a sharp sextet corresponding to α-Fe, in addition to a small contribution from a broad sextet corresponding to ϵ-Fe_3N, in agreement with XRD results. Thus from XRD and CEMS it can be seen that the system remain amorphous after annealing up to a temperature of 523 K. Therefore for self-diffusion measurements we choose 523 K as an upper limit of annealing temperature. It was found that even after the highest diffusion annealing temperature and time the film remained in the amorphous state.

The diffusion annealings of the samples were performed in a vacuum furnace with a base vacuum better than 10^{-6} Torr. The temperature in the furnace was controlled with an accuracy of ± 1.5 K. For diffusion measurements the concentration depth profile was measured by a secondary-ion

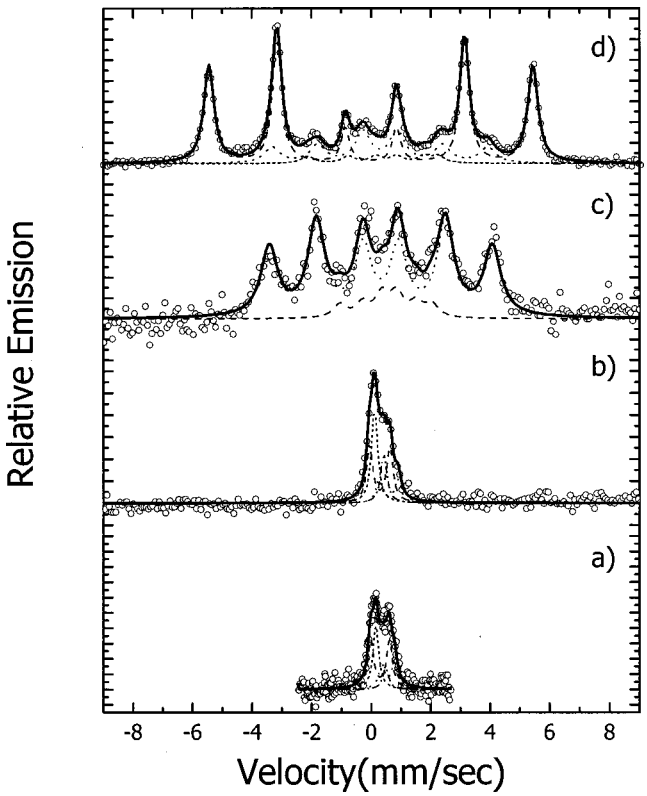

FIG. 3. The conversion-electron Mössbauer spectrum of the film (a) as-deposited and (b) annealed in vacuum at 523 K, (c) at 593 K, and (d) at 723 K. The full circles are experimental data points and the solid lines are fit to them.

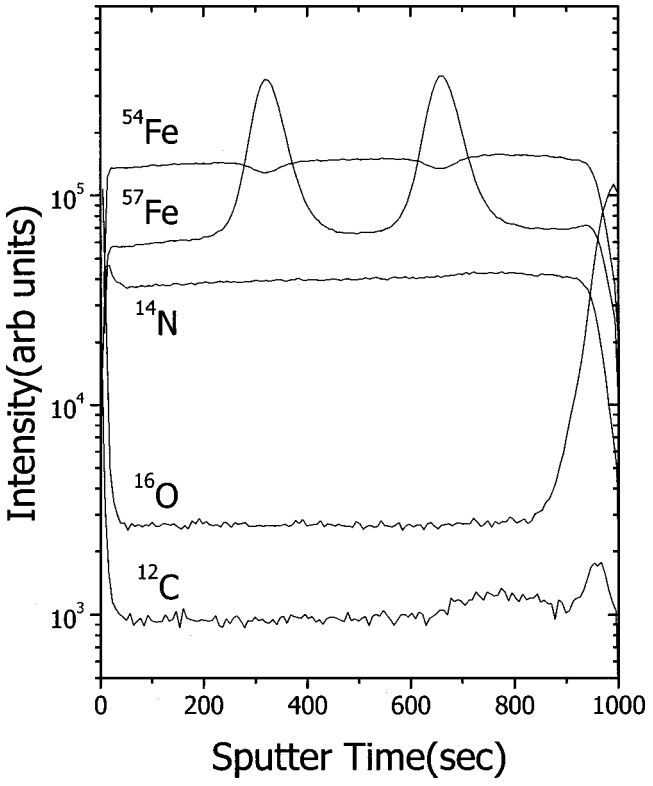

FIG. 4. SIMS depth profile of the as-deposited film.

mass CAMECA-IMS5F spectrometer. The primary ions used for sputtering were Cs^+ ions of energy 5.5 KeV and the ion current was about 15 nA. The secondary ions were detected by a double focusing magnetic mass spectrometer. Figure 4 shows the depth profile of ^{57}Fe, ^{54}Fe, nitrogen, oxygen, and carbon in the as-deposited film. ^{57}Fe shows two peaks of almost equal intensity, whereas ^{54}Fe shows dips at those two positions. The nitrogen profile does not show any change in intensity with depth, which again indicates (in agreement with the XRR results) that the nitrogen stoichiometry is uniform throughout the depth of the film. The oxygen and carbon contents in the film are sufficiently low and do not show any variation in their depth profiles.

From Fig. 4 it may be noted that depth profiles of ^{57}Fe are somewhat skewed towards higher sputtering time. This asymmetry in the depth profiles is due to radiation damage and small intermixing induced by the 5.5-keV Cs^+ ions used

TABLE I. Hyperfine parameters for the as-deposited and subsequently annealed FeN films. IS is the isomer shift relative to *a*-iron, while QS denotes the quadrupole splitting.

Sample	Phase	Site	H_{int} (T)	IS (mm/sec)	QS (mm/sec)	Relative area (%)
As deposited	Amorphous	Singlet1		0.48		9
		Singlet2		0.15		27
		Doublet1		0.30	0.62	41
		Doublet2		0.56	0.43	22
Annealed at 523 K	Amorphous	Singlet1		0.42		16
		Singlet2		0.12		31
		Doublet1		0.29	0.68	37
		Doublet2		0.58	0.60	15
Annealed at 593 K	ε-Fe_3N	Sextet1	9.6	0.55		14
		Sextet1	23.2	0.32		86
Annealed at 723 K	α-Fe	Sextet	33.7	−0.01	0.01	66
	ε-Fe_3N	Sextet	22.5	0.11	0.6	27
		Sextet	13.6	0.28	−0.5	7

for sputtering the samples.[23,26] A correction for this irradiation broadening of the profiles is applied to the primary concentration profiles using a procedure described in Refs. 23 and 26. The concentration profiles are corrected to yield the true ones according to the following equation:

$$c_r(x+h)=c_a(x)+h\frac{dc_a(x)}{dx}, \tag{1}$$

where $c_a(x)$ and $c_r(x)$ are the experimentally determined and true profiles, respectively, and h is a parameter that represents strength of intermixing due to Cs^+-ion bombardment. The value of h was determined by applying this correction on the as-deposited samples with the known concentration profile. The same value of h was used for correcting the depth profiles of the samples annealed for different periods of time.

For determining the diffusion augmented broadening of the depth profiles, isothermal annealings of the films were performed at temperatures 430, 450, 480, and 498 K for different times. The annealing times at lower temperatures are large as compared to higher temperatures. A typical broadening of the depth profile of ^{57}Fe as a function of annealing time at 450 K is shown in Fig. 5. The profiles have already been corrected for the Cs^+-ion irradiation broadening. In the present case, the thin-film solution to Fick's law can be applied and the tracer concentration of ^{57}Fe as a function of penetration depth x is given by[24]

$$c(x,t)=\frac{\text{const}}{2\sqrt{\pi Dt}}\exp[-(x^2/4Dt)], \tag{2}$$

where t is the time for annealing and D is the diffusion coefficient. Accordingly the profiles were fitted to Gaussians and the diffusion coefficients were calculated using the equation:[26]

$$\langle D\rangle(t)=\frac{\sigma_t^2-\sigma_0^2}{2t}, \tag{3}$$

where $\langle D\rangle(t)=(1/t)\int_0^t D(t')dt'$ is the time-averaged diffusion coefficient and σ_t is the standard deviation of the Gaussian depth profile obtained after an annealing time of t.

Figure 6 gives the diffusion coefficient at 450 K as a function of annealing time. One may note that initially the diffusion is fast, which decreases with annealing time. Such an annealing time dependence of the diffusion coefficient is attributed to structural relaxation in metallic glasses;[25,26] the as-deposited structure contains large concentration of structural defects characterized by excess free volume. With annealing the excess free volume is removed and the structure relaxes to thermal equilibrium glassy state. The observed time dependent $\langle D\rangle(t)$ was fitted assuming an exponential law for the relaxation of the diffusion coefficient,[25,26] so that

$$\langle D\rangle(t)=\frac{A\tau}{t}(1-e^{-t/\tau})+D_{\mathrm{SR}}. \tag{4}$$

Here D_{SR} is diffusivity in the structurally relaxed state and $A+D_{\mathrm{SR}}$ gives the diffusivity at the initial time ($t=0$), and τ is structural relaxation time. In Fig. 6, the solid line gives a fit of the measured data yielding the value of A, τ, and D_{SR}.

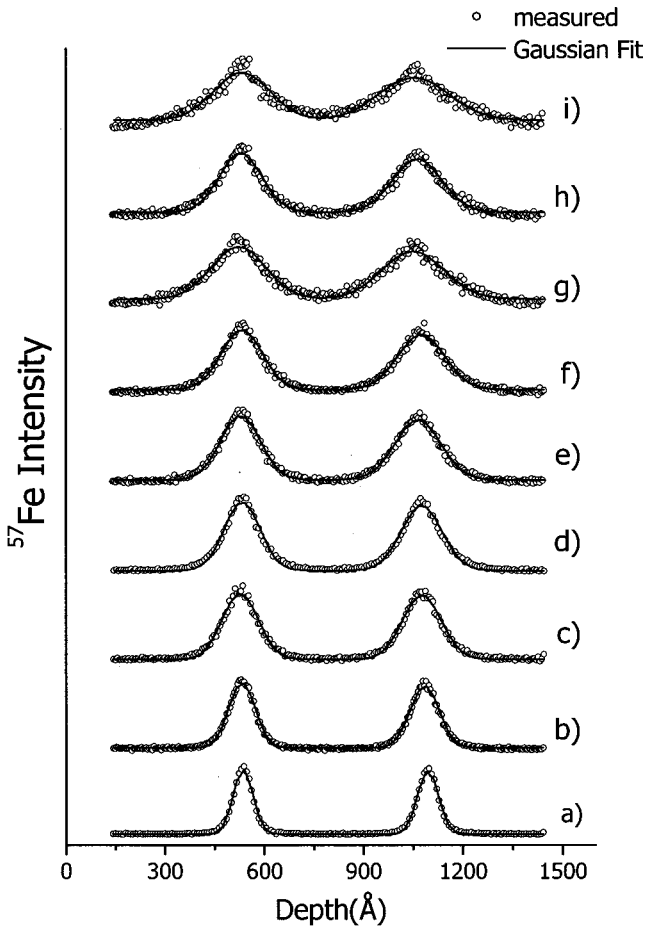

FIG. 5. Diffusion broadening of the SIMS depth profile after annealing at 450 K at different times (a) as-deposited, (b) 60 min, (c) 200 min, (d) 300 min, (e) 400 min, (f) 500 min, (g) 700 min, (h) 1300 min, and (i) 1900 min. The profiles have already been corrected for the Cs^+-ion broadening according to Eq. (1).

The values of diffusion coefficient in the structurally relaxed state obtained at four different temperatures were used to calculate activation energy and preexponential factor using the equation $D_{\mathrm{SR}}=D_0\exp(-q/k_BT)$, where D_0, q, and T

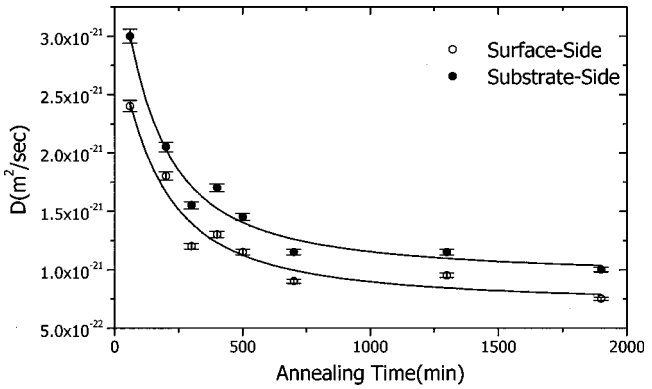

FIG. 6. Structural relaxation of the diffusion coefficient in the amorphous iron nitride thin film at 450 K.

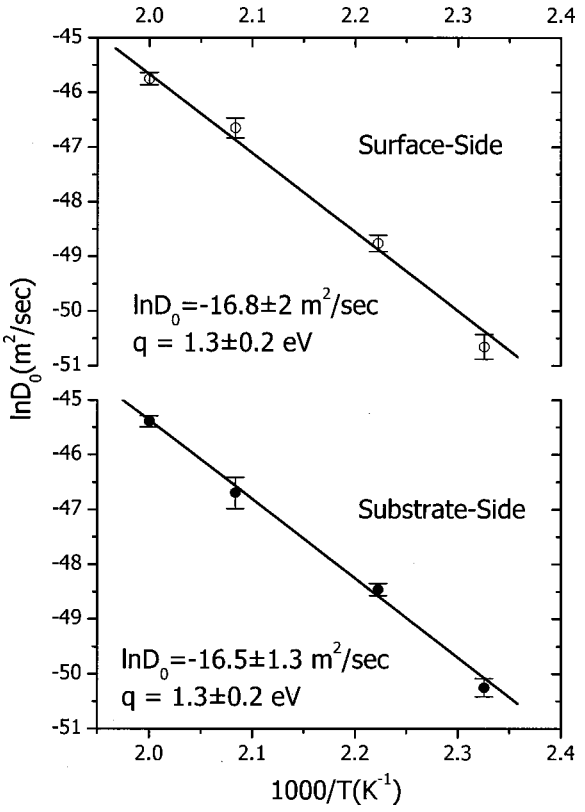

FIG. 7. Arrhenius behavior of diffusion coefficient with isothermal annealing temperature.

are the preexponential factor, activation energy, and annealing temperature, respectively. Figure 7 shows the plot of natural logarithm of diffusion coefficient versus the inverse of temperature, and it follows an Arrhenius behavior. The calculated values of $\ln D_0$ and the activation energy q for the depth profiles of the two marker layers are $\ln D_0 = -16.8 \pm 2\ \mathrm{m^2/sec}$; $q = 1.3 \pm 0.2$ eV and $\ln D_0 = -16.5 \pm 1.3\ \mathrm{m^2/sec}$; $q = 1.3 \pm 0.2$ eV, respectively.

A survey of the literature on self-diffusion in the metallic glasses shows that the activation energy of 1.3 eV for the present case is quite low as compared to that in other metallic glasses, especially TM-*M* systems. It may be noted that most of the diffusion studies in TM-*M* metallic glasses reported in the literature are on the system around the eutectic composition, thus having low metalloid concentration. Amorphous alloys over a wide range of metalloid concentration have been prepared using co-sputtering;[27] however, such systems can be prepared only in thin-film form and have not been used for diffusion measurement.

In the dense random packing model for the metallic glasses, the metal atoms form a dense random packing structure and the metalloid atoms occupy the interstitial sites in these structures.[28] It has been argued that TM-*M* systems have high stability around a metalloid composition of ~20 at. % as around this composition most of the interstitial sites are occupied by metalloid atoms.[28] For higher metalloid concentration strains will be created in the network of transition-metal atoms in order to accommodate the additional metalloid atoms, and some of the metalloid atoms may even occupy transition-metal sites. This results in a reduced stability of the amorphous phase. In the present case nitrogen has a concentration of about 40 at. %, which is substantially higher than 20 at. %, which can be incorporated in the interstitial sites, and thus will create strain in the iron network. It may be noted that the Fe-Fe nearest-neighbor (NN) distance in the system, as obtained from XRD measurements is 2.86 Å as compared to 2.5 Å observed in most of the TM-*M* metallic glasses around $TM_{80}M_{20}$ compositions. This larger Fe-Fe NN distance may be attributed to the strains created in the iron network in order to incorporate additional nitrogen atoms and due to some nitrogen atoms going substitutionally on iron sites. An increased Fe-Fe NN distance would also result in lowering of the mass density, which should vary as $1/a^3$, a being the NN distance. In addition, the mass density would also depend upon the average coordination number. In the present case the mass density as obtained from the x-ray reflectivity measurements is 6.2 g/cm^3 as compared to a typical mass density of 7.7 g/cm^3 for eutectic metal-metalloid systems.[29] If one assumes that reduced mass density in the present case is due to increased Fe-Fe NN distance then the ratio of the mass density of $FeN_{0.7}$ to that of a typical metallic glass (MG) should be proportional to the ratio of the cube of their NN distance, i.e., $d_{\mathrm{FeN}_{0.7}}/d_{\mathrm{MG}} = a^3_{\mathrm{MG}}/a^3_{\mathrm{FeN}_{0.7}} = 0.7$, this ratio is obtained by neglecting the mass of the nonmetal atoms. Since in the present case concentration of nonmetal atoms is almost double of that in a typical metallic glass, the actual ratio of the mass density would be a little more than 0.7. Thus the calculated mass density ratio agrees reasonably well with the experimental ratio of $6.2/7.7 = 0.8$. This suggests that a lower mass density in $FeN_{0.7}$ can be accounted for by a change in the Fe-Fe NN distance alone, implying that the average coordination number is similar to that in a typical metallic glass. A larger Fe-Fe NN distance would facilitate the atomic diffusion in the system. On the other hand, a stronger Fe-N bonding would tend to hinder the atomic diffusion. The observed value of activation energy in the present case is a result of an interplay between these two factors.

In a number of studies[9,10,11,12] it has been suggested that there exists a definite correlation between the natural logarithm of the preexponential factor and activation energy for

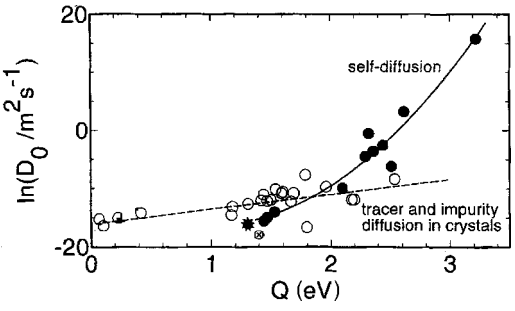

FIG. 8. Correlation between the natural logarithm of the prefactor, $\ln D_0$ and effective activation energy q, of diffusion coefficient in selected amorphous alloys (●) and in crystalline alloys (○) from Ref. 12. The crossed circle represents data from Ref. 4 and the star represents the values corresponding to the present study.

atomic diffusion in amorphous as well as crystalline solids. Sharma, Macht, and Naundorf[9] showed that an almost linear correlation exists between $\ln D_0$ and q for the diffusion of impurity atoms as well as self-diffusion in a number of metal-metal amorphous alloys. It may be noted that in case of an impurity atom diffusion, a number of factors such as atomic size and chemical affinity between impurity and host atoms may significantly affect the diffusion, thus making the situation more complicated. Therefore it is more meaningful to study the systematics of self-diffusion, in which case the influence of such factors is absent. In a more recent study Naundorf *et al.*[12] found that a well-defined correlation exists between $\ln D_0$ and q for self-diffusion of amorphous alloys, including both metal-metal and TM-*M* systems. A distinctly different correlation between $\ln D_0$ and q are observed for diffusion in crystalline and amorphous alloys. This correlation is regarded as key information to determine the validity of different diffusion models proposed for disordered structures. Figure 8 shows the data on the correlation between $\ln D_0$ and q taken from Ref. 12, to which self-diffusion data obtained more recently[4] has also been added. The point corresponding to the present measurement is shown by a star. It may be noted that point corresponding to the present system lies very well on the correlation line for the self-diffusion in amorphous alloys. This suggests that even in the present system the diffusion mechanism is very similar to that in other metallic glasses, although the present system has much stronger covalent bonds and also the concentration of the nonmetallic atoms is much higher.

In conclusion, self-diffusion of iron in amorphous iron nitride is studied using secondary-ion mass spectroscopy depth profiling of $^{57}FeN_{0.7}$ in $FeN_{0.7}$ films. The system shows structural relaxation behavior typical of metallic glasses. The values of the NN distance as obtained from XRD and the mass density obtained from XRR suggest that the structure of the amorphous $FeN_{0.7}$ system is rather similar to other TM-*M* glasses. The values of the preexponential factor D_0 and activation energy q are $\ln D_0 = -16.6 \pm 2\ m^2/sec$, $q = 1.3 \pm 0.2$ eV for this system. The mechanism of self-diffusion of iron in amorphous iron nitride is found to be very similar to metallic glasses.

The authors would like to acknowledge the help received from Mr. A. K. Balamurugan during SIMS measurements.

*Corresponding author. Email address: agupta@iucindore.ernet.in

[1] A. Heesemann, V. Zöllmer, K. Rätzke, and F. Faupel, Phys. Rev. Lett. **84**, 1467 (2000).
[2] K. N. Tu and T. C. Chou, Phys. Rev. Lett. **61**, 1863 (1988).
[3] A. Grandjean, P. Blanchard, and Y. Limoge, Phys. Rev. Lett. **78**, 697 (1997).
[4] P. Klugkist, K. Rätzke, S. Rehders, P. Troche, and F. Faupel, Phys. Rev. Lett. **80**, 3288 (1998).
[5] F. Faupel, P. W. Hüppe, and K. Rätzke, Phys. Rev. Lett. **65**, 1219 (1990).
[6] G. Ruitenberg, P. De Hey, F. Sommer, and Jilt Sietsma, Phys. Rev. Lett. **79**, 4830 (1997).
[7] P. W. Hüppe and F. Faupel, Phys. Rev. B **46**, 120 (1992).
[8] F. Speapen, J. Non-Cryst. Solids **31**, 207 (1978).
[9] S. K. Sharma, M.-P. Macht, and V. Naundorf, Phys. Rev. B **49**, 6655 (1994).
[10] S. K. Sharma, S. Banerjee, and A. K. Jain, J. Mater. Res. **4**, 603 (1989).
[11] H. Kronmüller and W. Frank, Radiat. Eff. Defects Solids **108**, 81 (1989).
[12] V. Naundorf, M.-P. Macht, A. S. Bakai, and N. Lazarev, J. Non-Cryst. Solids **250–252**, 679 (1999).
[13] K. Ratzke, A. Heesemann, and F. Faupel, J. Phys.: Condens. Matter **7**, 7633 (1995).
[14] G. Rummel and H. Mehrer, Phys. Status Solidi A **185**, 327 (1994).
[15] X.-P. Tang, U. Geyer, R. Busch, W. L. Johnson, and Y. Wu., Nature (London) **402**, 160 (1999).
[16] U. Geyer, S. Schneider, W. L. Johnson, Y. Qiu, T. A. Tombrello, and M.-P. Macht, Phys. Rev. Lett. **75**, 2364 (1995).
[17] H. Ehmler, A. Heesemann, K. Ratzke, F. Faupel, and U. Geyer, Phys. Rev. Lett. **80**, 4919 (1998).
[18] Mukul Gupta, Ajay Gupta, S. M. Chaudhari, D. M. Phase, V. Ganesan, M. V. Rama Rao, T. Shripathi, and B. A. Dasannacharya, Vacuum **60**, 399 (2001).
[19] F. H. Sanchez, Y. D. Zhang, and J. I. Budnick, Phys. Rev. B **38**, 8508 (1988).
[20] L. G. Parratt, Phys. Rev. **95**, 359 (1954).
[21] A. Guinier, *X-Ray Diffraction in Crystals, Imperfect Crystals, and Amorphous Bodies* (Dover, New York, 1994).
[22] T. Hinomura, Ph.D. thesis, Osaka University, Osaka, Japan, 1998.
[23] G. Brebee, R. Seguin, C. Sella, J. Bevenot, and J. C. Martin, Acta Metall. **28**, 327 (1980).
[24] P. G. Shewmon, *Diffusion in Solids* (McGraw-Hill, New York, 1963), p. 7.
[25] A. K. Tyagi, M.-P. Macht, and V. Naundorf, Acta Metall. Mater. **39**, 609 (1991).
[26] Y. Loirat, J. L. Boequet, and Y. Limoge, J. Non-Cryst. Solids **265**, 252 (2000).
[27] C. L. Chien, and K. M. Unruh, Phys. Rev. B **24**, 1556 (1981).
[28] D. E. Polk, Acta Metall. **40**, 485 (1972).
[29] R. Gerling and R. Wagner, Scr. Metall. **16**, 963 (1982).